

A Novel High-Performance Ti/ATONPs-MWCNTs Electrode Based on Screen Printing Technique for Degradation of C.I. Acid Red 73

Qiutong Xu, Xiaoliang, Song and Li Xu*

School of Chemical Engineering and Technology, Tianjin Key Laboratory of Membrane Science and Desalination Technology, Tianjin University, Tianjin 300072, P. R. China

*E-mail: xuli620@163.com

Received: 15 August 2017 / Accepted: 5 October 2017 / Online Published: 1 December 2017

A large effective surface area and a good electrical conductivity are very important characteristics for electrodes used in wastewater treatment. To improve them while lowering the cost, a novel MWCNTs-modified (Ti/ATONPs-MWCNTs) electrode was produced by a screen-printing technique. To test its performance, the electrode was compared to two other electrodes, namely, Ti/SnO₂-Sb and Ti/ATONPs. Several important electrochemical measurements including impedance spectroscopy (EIS), cyclic voltammetry (CV), chronocoulometry (CC) and linear sweep voltammetry (LSV), were used in this study. A toxic organic dye (C.I. Acid Red 73) was chosen as the target pollutant to test the degradation by the removal of chroma and chemical oxygen demand (COD). Compared to Ti/SnO₂-Sb and Ti/ATONPs, Ti/ATONPs-MWCNTs show the lowest charge transfer resistance (0.24 Ω), the largest effective surface area (61.97 cm²·cm⁻²) and the highest oxygen evolution potential (2.15 V). It is known that superior values of these performance characteristics are very important for improving the efficiency of wastewater decontamination. After 90 min electrolysis using Ti/ATONPs-MWCNTs, the removal of AR 73 reached 59.4%, while the energy consumption was as low as only 6.2 Wh·L⁻¹. The remnant COD was only 45% after 3 h of degradation, with an instantaneous current efficiency (ICE) over 80% obtained for Ti/ATONPs-MWCNTs. These results demonstrate the promising prospects for the use of the novel Ti/ATONPs-MWCNTs electrodes in wastewater treatment processes.

Keywords: Adsorption-electrocatalysis, ATO nanoparticles, Multi-walls carbon nanotubes, Screen printing, Azo dyes

1. INTRODUCTION

Since the wastewater containing synthetic organic dyes is toxic or carcinogenic for aquatic and terrestrial ecosystems, the large-scale generation of such wastewater has aroused great concern [1, 2]. It is obvious that azo dyes with the chromophore of -N=N- units are some of the most common dyes [3]. Therefore, efficient methods for the removal of such toxic pollutant have been developed to reduce

the impact of the azo dyes on the environment [4]. Electro-catalytic oxidation characterized by high oxidation efficiency, strong amenability and no secondary pollution can be used as an innovative alternative to control low-duty application, thus making this technique a good candidate for achieving the efficient removal of the azo dyes from wastewater [5].

During the electro-catalytic oxidation process, the anode plays an indispensable role in wastewater degradation. Recently, researchers have attempted to adjust the composition of the anode in order to improve its electrochemical activity and stability. Previously published studies have found that dimensionally stable anodes (DSAs) and carbon anodes show good performance in wastewater treatment [6]. Due to their good stability and catalytic activity, dimensionally stable anodes (DSAs), such as IrO_2 [7, 8], RuO_2 [8], PbO_2 [9, 10] and SnO_2 [11] have made rapid progress. Among these, SnO_2 and especially Sb-doped SnO_2 electrodes are considered to be relatively excellent for organic degradation, and have also been shown to be environmentally friendly. Carbon anodes, including active carbon electrodes, carbon nanotube electrodes (CNTs) and graphene electrodes have also attracted wide attention from researchers due to their diversity of textures/structures and surface chemistries. It was reported that activated carbon electrodes can be effectively designed and applied to the treatment of diclofenac sodium in water [12]. Additionally, the degradation of coking wastewater based on carbon nanotube electrodes (CNTs) has been used as a successful alternative to the treatments relying on traditional electrodes [13].

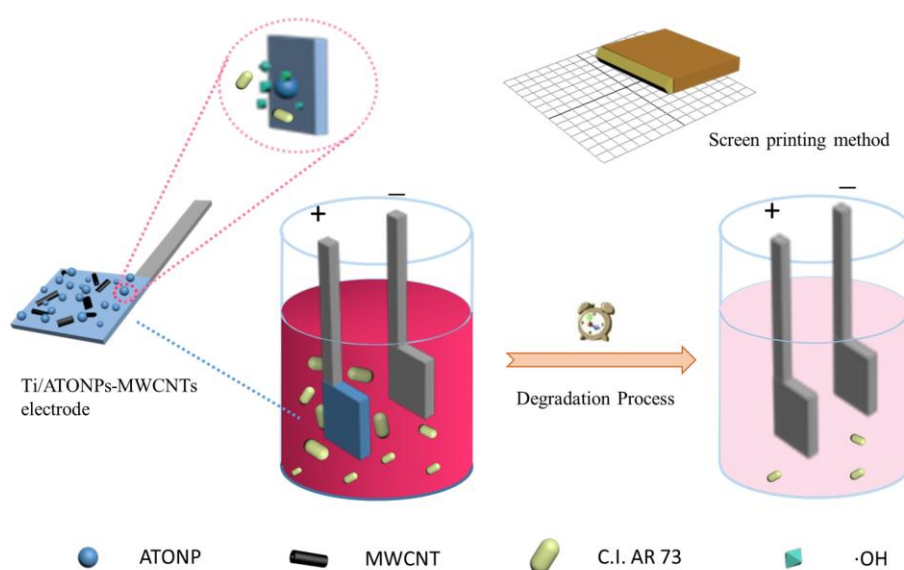
In fact, the current efficiency of Sb-doped SnO_2 electrodes decreases distinctly with the concentration loss of organic dyes. Due to physical adsorption and the synergistic effect on degradation, CNTs show excellent results at low concentrations. Based on this finding a new approach of preparing the anodes by combining the DSAs (Sb-doped SnO_2) with the carbon anodes (CNTs) can be considered in order to obtain bifunctional anodes with superior performance in wastewater treatment. Therefore, in the present work, multi-walls carbon nanotubes (MWCNTs) modified antimony tin oxide nanoparticles (ATONPs) electrodes on Ti substrates are fabricated in order to enhance the electro-catalytic oxidation. ATONPs is a form of solid powder with nanoparticles for Sb-doped SnO_2 that provides a prepared average particle size of the electrode coating and contributes to the novel preparation method mentioned in the next section. MWCNTs featuring large specific surface area, excellent electrical conductivity, high mechanical strength and stable electrochemical properties can provide more absorption sites, enhancing the electrical conductivity and mechanical strength during the process of catalytic degradation of organic pollutants. This contributes to the improvement of the degradation rate of organic wastewater and reduces the required electric energy consumption [14]. More importantly, it further shows that MWCNTs have good compatibility with ATONPs, making them quite attractive for use in practical applications.

To fabricate the novel Ti/ATONPs-MWCNTs electrodes, a screen-printing technique was applied in this work. Compared to the traditional fabrication methods such as spray pyrolysis [15], dipping [16], chemical vapour deposition [17], electrodeposition [18,19] and sol-gel process[20], screen printing, which prints the mixture of coating materials and binders onto the substrate through the screen, has solved some problems exhibited by the traditional methods. Screen printing enables the control of the surface morphology and the capacity of the catalyst layer, which is beneficial for its further development and application. Screen printing also enables accurate control of the nano-sized

grains of the coating, simplicity of operation and low cost, which are all highly required. Multi-walls carbon nanotubes (MWCNTs) modified ATONPs electrodes on Ti substrates fabricated by screen printing have not yet been applied to wastewater treatment. Consequently, screen printing is introduced in this paper to promote the use of the MWCNTs-modified ATONPs electrodes in wastewater treatment for the first time.

Based on our previous studies, Sb-doped SnO_2 electrodes were prepared with different dopants by adopting different methods. Zhang et al. [21] fabricated $\text{Ti}/\text{SnO}_2\text{-Sb}$ electrodes modified by carbon nanotubes by pulse electrochemical deposition, enhancing the degradation of dye wastewater. However, the CNT structure was destroyed and could not be observed in the image of the electrode specimen. Then, the screen-printing technique was first introduced to fabricate the Ti/ATONPs electrodes with nano-sized grains and a mesoporous structure [22]. Therefore, the Ti/ATONPs -MWCNTs electrodes are expected to enhance both the organic molecule absorption capacity and the electro-catalytic activity by adopting the screen-printing technique at a low electric energy cost.

In this work, we focused on determining whether the novel Ti/ATONPs -MWCNTs electrode prepared by screen printing has the morphology of nano-sized grains with the tubular structure of MWCNTs. We also examined whether the novel electrode shows lower energy consumption and better electro-catalytic performance as well as physical absorptive ability for the degradation of refractory organic pollutants. To characterize the surface morphology of the electrodes, scanning electron microscopy (SEM) was used for the images of the electrode coatings. In addition, cyclic voltammetry (CV), electrochemical impedance spectroscopy (EIS), chronocoulometry (CC) and linear sweep voltammetry (LSV) were also applied to study the electrochemical properties of Ti/ATONPs -MWCNTs. C.I. Acid Red 73, a typical azo dye, was chosen as the model organic pollutant to investigate the degradation capability on the basis of concentration measurement and chemical oxygen demand (COD) analysis (Scheme 1).



Scheme 1. Schematic representation of the electrode structure and mechanism of degradation. The novel adsorption-electrocatalysis anode combined the ATONPs with MWCNTs using the screen-printing technique. Under the action of constant current, C.I. AR 73 model wastewater was degraded until anodic inactivation

2. EXPERIMENTAL SECTION

2.1. Materials

C.I. Acid Red 73 (>99% purity), the structural parameters of which are shown in Table S1, was purchased from Qingdao Chuanlin Dyestuffs Co. Ltd., Shandong, China and used directly without any further purification. Antimony doped tin oxide nanoparticles (ATONPs) with a molar ratio of Sn/Sb equal to 9.65:1 ($\geq 99.5\%$ metals basis, 20~80 nm), terpineol ($C_{10}H_{18}O$) and ethyl cellulose were purchased from Aladdin, China. Multi-walled carbon nanotubes (MWCNTs) (>97% purity), with the diameter, length and specific area of 10~20 nm, less than 2 μm and 100~120 $m^2 \cdot g^{-1}$, respectively, were purchased from Nanotech Port CO. Ltd, Shenzhen, China. All other chemical reagents including H_2SO_4 , $C_2H_2O_4 \cdot 2H_2O$, NaOH, $CuSO_4 \cdot 5H_2O$, $(NH_4)_2SO_4$, $SnCl_2 \cdot 2H_2O$, $SbCl_3$, $NaSO_4$, diethylenetriamine, gelatine and sodium pyrophosphate tetrabasic decahydrate were analytical grade and were purchased from Tianjin Fuchen Chemical reagents factory, China. Deionized water with the resistivity near to 18.2 $M\Omega \cdot cm$ was purchased from Tianjin Ultrapure Co. and was used for the preparation of all solutions.

2.2 Electrode preparation

To prepare a good adhesive metal oxide coating, prior to the anodisation, the titanium substrates were pretreated as follows. First, Ti sheets were cut into rectangular shape with the dimensions of 20 × 20 mm and the thickness of 0.5 mm as the base material and polished with 320-grit sandpaper. Second, the sheets were degreased in 10 wt.% NaOH at 90°C for 1 h, and then etched in 5 wt.% oxalic acid at 99.5°C for 2 h after washing with deionized water to produce a surface with a uniform roughness. Finally, the treated sheets were kept in adequate absolute ethanol.

The Ti/ATONPs-MWCNTs electrodes were fabricated by screen printing. The detailed procedure for the fabrication of Ti/ATONPs-MWCNTs electrodes was as follows. The paste used for screen printing consisted of ethyl cellulose, terpineol, ATONPs and MWCNTs with the mass ratio of 1:3.5:1:0.02. A well-distributed paste was obtained after stirring for 3 h. Then, the Ti sheets were fixed on the printing platform matching with the mesh (20.5 × 20.5 mm) after washing and drying. The squeegee was attached to the screen and printing was performed linearly along the screen with the angle of 45° and a constant speed of 4 $mm \cdot s^{-1}$, thus forcing the distributed paste through the screen (mesh count = 325 $inch^{-1}$, mesh thickness = 48 μm , wire diameter = 28 μm) onto the Ti sheets. Subsequently, the electrodes were dried at 80°C for 10 min in the oven. Then, the same procedure was conducted again for the other side of the electrodes. The above operation was repeated 4 times to produce the Ti/ATONPs-MWCNTs electrodes, and in the final treatment, the sample was annealed for 2 h at 450°C at a heating rate of 1°C·min⁻¹.

For comparison, the coating of the Ti/ATONPs electrodes without the MWCNTs structure was prepared by screen printing via the same procedure as in the study by Xu et al. [22]. The Ti/ATONPs electrodes had the paste consisting of terpineol, ethyl cellulose and ATONPs with the mass ratio of 3.5:0.5:1 and the electrodes were annealed for 2 h at 500°C for the final heat treatment. The traditional

Ti/SnO₂-Sb electrodes were fabricated by direct current electrodeposition as in our previous work [22]. Primarily, Cu was deposited on the treated Ti sheets at 20 mA·cm⁻² at room temperature for 15 min in an aqueous solution with 100 g·L⁻¹ CuSO₄·5H₂O, 20 g·L⁻¹ (NH₄)₂SO₄ and 40 mL·L⁻¹ DETA [23]. The electrodeposition was subsequently carried out for 90 min in a Sn-Sb electrodeposition bath consisting of Na₄P₂O₇·H₂O, 115 g·L⁻¹; C₄H₆O₆, 7 g·L⁻¹; SnCl₂·2H₂O, 30 g·L⁻¹; SbCl₃, 3.14 g·L⁻¹; and gelatine, 0.4 g·L⁻¹. The Sn/Sb molar ratio in Ti/SnO₂-Sb electrodes is equal to that in ATONPs as obtained from a commercial source. Then, the electrodes were annealed at 500°C for 2 h at the heating rate of 10°C·min⁻¹.

Notably, the novel MWCNTs-modified ATO nanoparticles electrodes produced by screen printing were named Ti/ATONPs-MWCNTs in order to distinguish them from the traditional Ti/SnO₂-Sb and Ti/ATONPs obtained by screen printing.

2.3. Characterization of the electrodes

The morphological images of Ti/ATONPs-MWCNTs, Ti/ATONPs and Ti/SnO₂-Sb electrodes were obtained by field emission scanning electron microscopy (FE-SEM, S-4800, Hitachi, Japan). Electrochemical experiments were carried out in a conventional three-electrode cell system at an electrochemical workstation (PARSTAT 2273, PARC, USA). A platinum foil (4 × 4 cm) was employed as the counter electrode, and the Ag/AgCl/0.1 M KCl was used as the reference electrode, while our prepared electrodes (Ti/ATONPs-MWCNTs, Ti/ATONPs and Ti/SnO₂-Sb) were applied as the working electrodes. All potentials were in reference to Ag/AgCl/0.1 M KCl, unless stated otherwise. Electrochemical impedance spectroscopy (EIS) was performed to test the electrical conductivity of the electrodes at the open circuit potential with the frequency range of 5×10⁴~5×10⁻² Hz and amplitude of 10 mV. Further electrochemical properties testing was performed by cyclic voltammetry (CV) at the scan rate of 50 mV·s⁻¹ with the scan range from 0.3 to 1.5 V. The two characterizations described above were both performed in an aqueous solution of 0.5 M H₂SO₄. The chronocoulometry (CC) method can be chosen to determine the electrochemically effective surface areas of electrodes, using 0.1 mM K₃[Fe(CN)₆] as the model complex and 1 M KCl as the electrolyte [24]. The oxygen evolution potentials (OEP) of the electrodes were examined by the linear sweep voltammetry (LSV) at 10 mV s⁻¹ with the range from 1.0 to 2.5 V in 0.1 M Na₂SO₄.

2.4. Degradation of AR 73

C.I. Acid Red 73 was selected as a model dye in wastewater to test the ability of organic degradation. Adsorption studies were conducted in 100 mL cylindrical vessels with 0.1 g·L⁻¹ AR 73 solution shaken at 80 rpm at room temperature for 2 h. 1 mL of the samples were extracted and then analysed for contaminant concentration. Meanwhile, the electrochemistry catalytic ability tests were carried out in an aqueous solution of 0.5 g·L⁻¹ AR 73 with 0.1 M Na₂SO₄ as the supporting electrolyte under galvanostatic control of 20 mA·cm⁻² at room temperature. A DC potentiostat with the voltage range of 0~32 V was employed as the power supply for degradation experiments. Ti/ATONPs-

MWCNTs, Ti/ATONPs or Ti/SnO₂-Sb were used as the anode and a pretreated titanium plate with the same dimensions of 20 × 20 mm was used as the cathode. The solutions were sampled by 1 mL at the same time interval of 15 min for the degradation test and 2 mL at the same time interval of 30 min for chemical oxygen demand (COD) analysis.

The contaminant concentration and chroma were monitored using a UV-Visible absorption spectrophotometer (UV-1000, Shanghai, Tianmei Scientific Instruments Co., China) with the absorbance measurements between 200 and 600 nm. The COD values were measured using the COD reactor and a spectrophotometer (DR1010 COD, HACH, USA).

3. RESULTS AND DISCUSSION

3.1. Structure and morphology of the electrode coatings

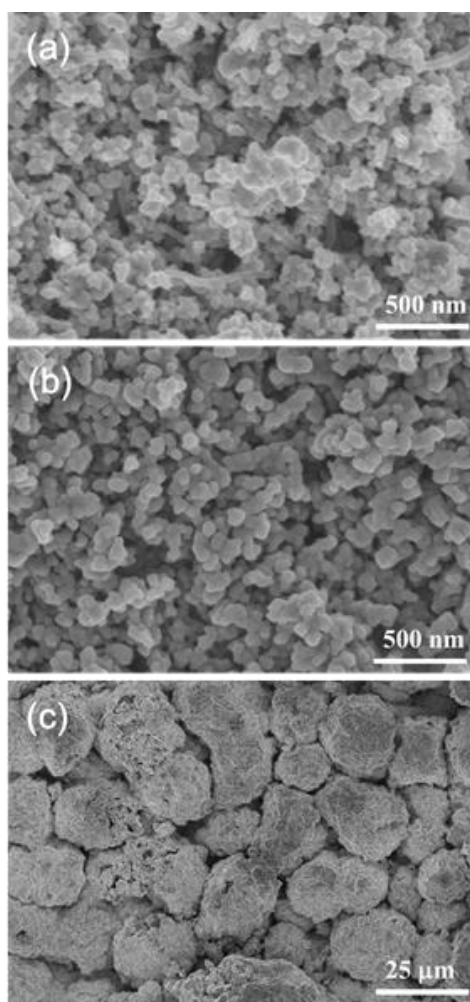


Figure 1. SEM images of Ti/ATONPs-MWCNTs (a), Ti/ATONPs (b) and Ti/SnO₂-Sb (c).

The Ti/ATONPs-MWCNTs electrodes were prepared by the screen-printing technique. As mentioned above, preparation of the paste containing MWCNTs is the key step for this technique. MWCNTs were treated by ultrasonication in an ethanol solution for 2 h and then were dried at a constant temperature (80 °C). Finally, MWCNTs were homogeneous diffused in the precursor paste

[25]. The SEM images mapping the as-prepared Ti/ATONPs-MWCNTs, Ti/ATONPs and Ti/SnO₂-Sb are shown in Figure 1. There are some cracks on the surface due to the thermal treatment, which could be explained by the heat-expansion and cold-contraction effects. The coating micromorphologies show a porous structure that shows the increase of the real surface area compared to bulk samples.

The Ti/ATONPs-MWCNTs and Ti/ATONPs electrodes fabricated by the screen printing technique both show the mean grain size of almost 50 nm. In comparison, the mean grain size of the Ti/SnO₂-Sb electrodes fabricated by electrodeposition is approximately 20 μm , which is far larger than that of other two kinds of electrodes. To the best of our knowledge, the larger grain size always corresponds to the smaller amount of active sites, which may weaken the degradation. Moreover, several pipes of MWCNTs can be clearly observed in Figure 1a. Thus, the addition of MWCNTs can enhance the mechanical properties, conductivity and thermodynamics of the electrodes [13]. Such small grain sizes and porous structure of MWCNT pipes could increase the specific surface area of the catalyst layer and provide more active sites for electro-catalytic oxidation [26].

3.2. Electrochemical properties of the electrodes

3.2.1. Electrochemical impedance spectroscopy (EIS)

It is widely believed that electrochemical impedance is related to the surface morphology and microstructure inside the catalyst layer of the electrodes. Electrochemical impedance spectroscopy (EIS) measurements have been widely applied to study the electrochemical properties, providing much information regarding the morphology and kinetics of the electrodes. In this study, the Randall equivalent circuit was employed to fit the impedance spectra obtained for the Ti/SnO₂-Sb electrodes, as shown in Figure 2a [27]. The circuit contains four components, namely, the uncompensated electrolyte resistance between working and reference electrodes (R_s), the double-layer capacitance (C_{dl}), the charge transfer resistance (R_{ct}) and the Warburg impedance (Z_w). Figure 2b shows that a component of the constant phase element (CPE) was used to replace the double-layer capacitance (C_{dl}) in order to form an equivalent circuit. CPE is suitable for Ti/ATONPs-MWCNTs and Ti/ATONPs electrodes with mesoporous structure fabricated by screen printing [28]. All Nyquist plots of the prepared electrodes consisted of a semicircle related to a charge transfer controlled process in the high-frequency region, and a skew line with the low positive correlation with the charge transfer resistance (R_{ct}).

According to the plots shown in Figure 2c, the semicircular diameter of the Ti/SnO₂-Sb electrode was obviously larger than those of the electrodes fabricated by the screen printing technique, and the R_{ct} of 13.24 Ω was obtained by the fit [29]. The magnified schematic diagram of the outstanding area in Figure 2c is shown in Figure 2d, where we can distinctly observe the Nyquist curves of the Ti/ATONPs-MWCNTs and Ti/ATONPs electrodes. According to the fitting results in Figure 2d, the R_{ct} values of Ti/ATONPs-MWCNTs and Ti/ATONPs were 0.24 Ω and 0.47 Ω , respectively. This showed that the use of the screen-printing technique decreased the impedance by almost two orders of magnitude [30]. Compared to Ti/ATONPs, the addition of MWCNTs decreased the charge transfer resistance (R_{ct}) by almost 50%. Herein, due to the excellent conductivity of the

MWCNT, the Ti/ATONPs-MWCNTs electrodes have shown the advantages of low charge transfer resistance and fast electron transfer speed. These may enhance the wastewater degradation ability and reduce energy consumption, as described below.

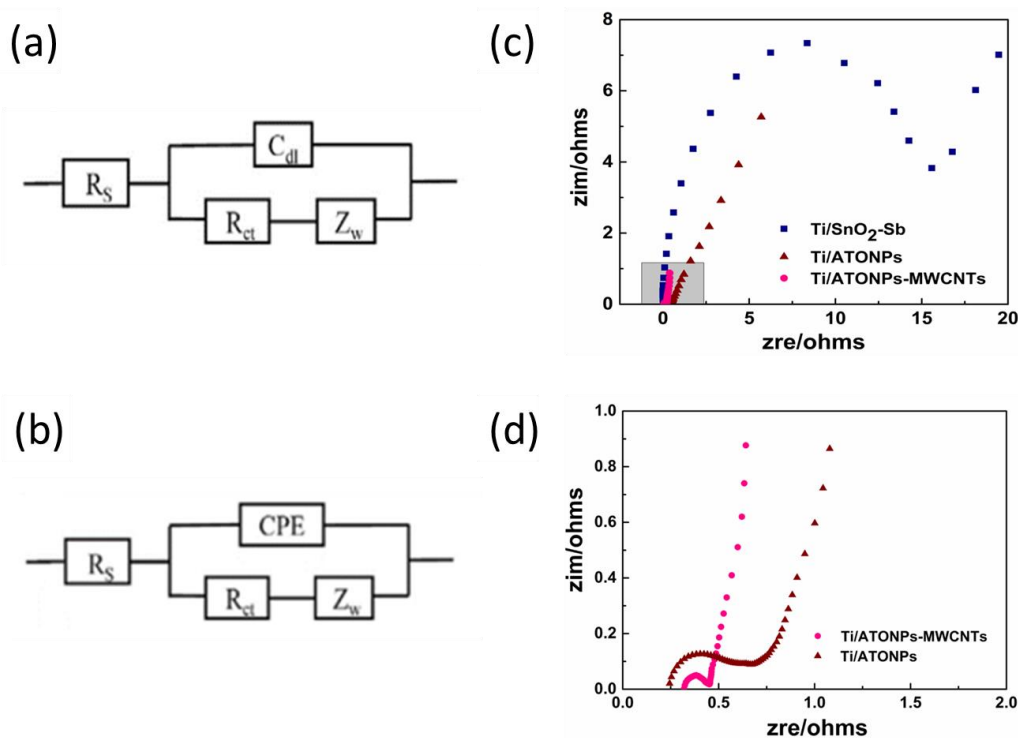


Figure 2. Equivalent circuit model for Ti/SnO₂-Sb (a), Ti/ATONPs-MWCNTs or Ti/ATONPs (b), and electrochemical impedance spectroscopy complex plane plots (c, d).

3.2.2 Cyclic voltammetry (CV)

Cyclic voltammetry measurements were performed to determine the electrochemical properties in a further investigation of the performance of the anodic layers based on the three kinds of electrodes. Figure 3 clearly shows that no redox peak is observed in the curves of the electrodes, indicating that all electrodes were non-active electrodes in the selected scanning region [31]. All CV curves at the same scan rates showed quasi-rectangular shapes. Remarkably, among these electrodes with various anodic layers, Ti/ATONPs-MWCNTs exhibited the largest separation between the levelled anodic and cathodic currents, indicating larger specific capacitances [32]. This suggests that Ti/ATONPs-MWCNTs is electrochemically more accessible, which is crucial for electro-catalytic reactions. By contrast, Ti/SnO₂-Sb and Ti/ATONPs exhibit comparatively lower specific capacitances evaluated under the same test conditions, owing to their extensive agglomeration and fewer catalytic sites. The CV tests suggested that the electrochemical accessible surface area increased remarkably due to the large specific surface area of MWCNTs, resulting in the significant improvement of the specific capacitance compared to the Ti/SnO₂-Sb and Ti/ATONPs [33].

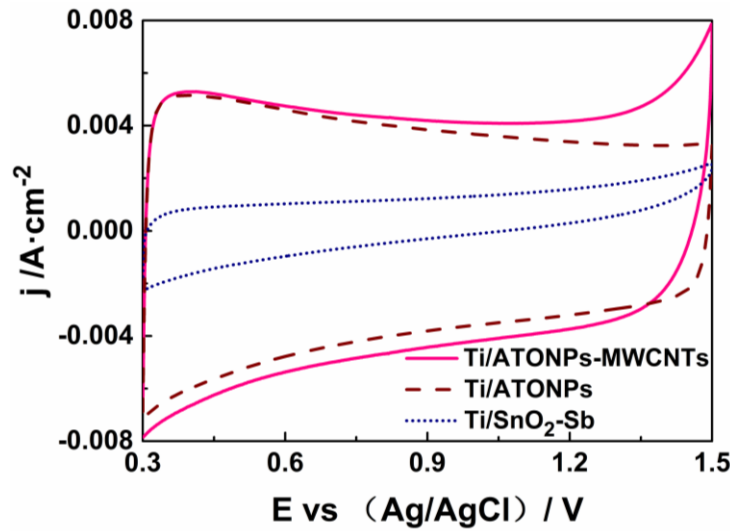


Figure 3. Cyclic voltammograms of different electrodes in 0.5 M H₂SO₄ solution at scan rate of 50 mV·s⁻¹.

3.2.3. Chronocoulometry (CC)

Chronocoulometry is an accurate electrochemical technique that can effectively study the phenomenon of adsorption on the electrode surface. The electrochemical effective surface areas (*A*) during the reaction time of the anodes can be investigated by chronocoulometry (Figure 4). In this study, 0.1 mM K₃[Fe(CN)₆] was chosen as the model complex (the diffusion coefficient of K₃[Fe(CN)₆] in 1 M KCl is 7.6×10⁻⁶ cm²·s⁻¹). The *A* value was determined in accordance with Anson's law [34]:

$$Q(t) = 2nFAc \frac{D^{1/2}}{\pi^{1/2}} t^{1/2} + Q_{dl} + Q_{ads} \quad (1)$$

where *n* is the electron transfer number, *F* (C·mol⁻¹) is the Faraday constant, *c* (mol·cm⁻³) is the substrate concentration, *D* (cm²·s⁻¹) is the diffusion coefficient, *Q_{dl}* (C) is the double-layer charge, which can be eliminated by background subtraction, and *Q_{ads}* (C) is the Faradic charge [35]. According to the results shown in Figure S1, the curve slopes of *Q* versus *t*^{1/2} were 7.44×10⁻³ C·s^{-1/2} (Ti/ATONPs-MWCNTs), 4.68×10⁻³ C·s^{-1/2} (Ti/ATONPs) and 3.65×10⁻³ C·s^{-1/2} (Ti/SnO₂-Sb), respectively. Based on the Anson equation, the corresponding *A* values were calculated as 61.97 cm²·cm⁻², 38.98 cm²·cm⁻² and 3.04 cm²·cm⁻², respectively. Therefore, the electrochemical effective surface area of the electrodes modified with MWCNTs were obviously increased, benefiting from the morphology of the nano-sized grains with a mesoporous structure and the structure of MWCNTs. This results in an improvement of the electrochemical oxidation capability and in the increased AR 73 adsorption onto the surface.

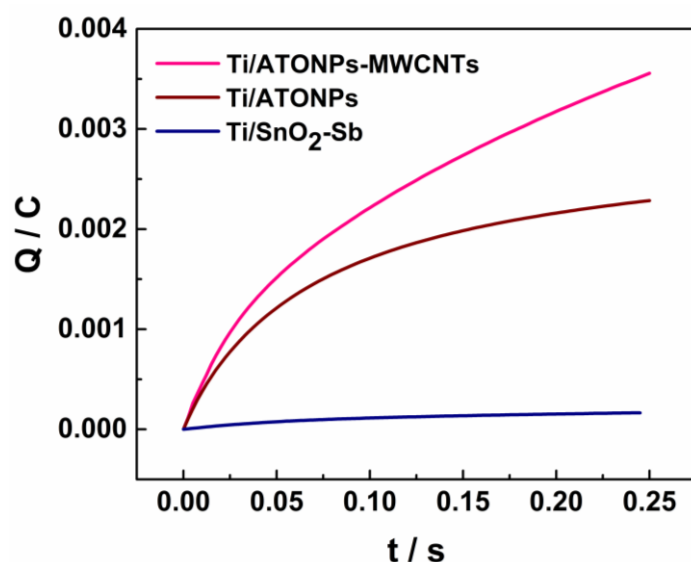


Figure 4. Plot of Q - t curve in 0.1 mM $K_3[Fe(CN)_6]$ containing 1 M KCl for different electrodes.

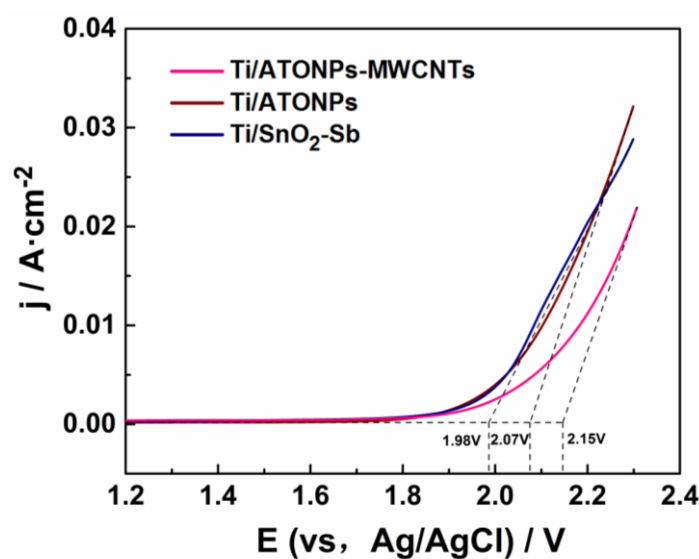


Figure 5. Linear sweep voltammetric curves in 0.1 M Na_2SO_4 solution at scan rates of $10 \text{ mV} \cdot \text{s}^{-1}$ for different electrodes.

3.2.4. Linear sweep voltammetry measurements (LSV)

The oxygen evolution potential (OEP), which is the potential when the electrode is involved in the oxygen evolution reaction (OER), can characterize the difficulty of the oxygen evolution reaction for the electrodes. A High OEP is advantageous for restraining the occurrence of side reactions, enhancing the organic degradation ability and weakening the influence of oxygen to peel the catalyst layer. Therefore, the OEP is positively correlated with the organic degradation ability of the anodes. To further study the differences between the three kinds of anodes, linear sweep voltammetry (LSV) curves were investigated to examine the OEPs of the three electrodes. As expected, the polarization curve of Ti/ATONPs-MWCNTs exhibits a much higher OER onset potential ($\approx 2.15 \text{ V}$ vs Ag/AgCl)

and a smaller catalytic current compared to Ti/ATONPs (≈ 2.07 V) and Ti/SnO₂-Sb (≈ 1.98 V) in the same test conditions, as shown in Figure 5. Here, Ti/ATONPs-MWCNTs showed a higher OEP owing to the structure of MWCNTs and the catalytic layer nano-sized grains, resulting in a better degradation of AR 73 and lower energy consumption, as described below.

3.3. Physical adsorptive properties of the electrodes

As a kind of porous material, MWCNTs display a physical adsorption capability. Moreover, previous studies indicated that the adsorption sites of MWCNTs mainly exist in the cylindrical external surface or are present between the MWCNTs tubes [36]. In this study, an aqueous solution of 0.1 g·L⁻¹ AR 73 was chosen as model wastewater in physical adsorption experiments, with the experimental results shown in Figure S2. Without an electric current, after a 120-min treatment on these electrodes, the removal of AR 73 on Ti/ATONPs-MWCNTs, Ti/ATONPs and Ti/SnO₂-Sb reached 18.7%, 4.2% and 2.3%, respectively. The Ti/ATONPs and Ti/SnO₂-Sb electrodes, owing to their small grain sizes, showed little physical adsorption. However, the electrodes modified with MWCNTs (Ti/ATONPs-MWCNTs) demonstrated the best physical adsorption performance among these electrodes due to the porous structure of the external surface on the MWCNTs.

3.4. Electrochemical degradation of AR 73 on the electrodes

Figure 6 shows the degradation rate of AR 73 and the semilog relationship of AR 73 chroma versus the electrolysis time (See Figure 6 inset) on Ti/ATONPs-MWCNTs, Ti/ATONPs and Ti/SnO₂-Sb electrodes in a 0.5 g·L⁻¹ AR 73 solution. After 90 min of electrolysis, AR 73 removal on Ti/ATONPs-MWCNTs was 59.4%, while the corresponding removals on Ti/ATONPs and Ti/SnO₂-Sb were 52.1% and 44.5%, respectively, under the same current density (20 mA·cm⁻²). The degradation of AR 73 followed pseudo-first-order kinetics, and the values of the rate constant (k) were given by:

$$\ln \frac{C_0}{C_t} = kt \quad (2)$$

where C_0 is the initial concentration of AR 73, C_t is the concentration of AR 73 at a given time (t), and k is the kinetic rate constant, which we need to calculate. As shown in Figure 6, the k indices were 0.579 h⁻¹, 0.488 h⁻¹ and 0.385 h⁻¹ for the Ti/ATONPs-MWCNTs, Ti/ATONPs and Ti/SnO₂-Sb electrodes, respectively. Apparently, the rate of the kinetics for Ti/ATONPs-MWCNTs electrodes was increased significantly according to the results of the degradation rate. This result implied that AR 73 could be degraded more rapidly on Ti/ATONPs-MWCNTs owing to the lower electrochemical impedance, larger electrochemical effective surface area and more active adsorption in the coating.

The chemical oxygen demand (COD) is an indicator of the amount of the reducing agent in the wastewater, which is expressed by the dosage of a strong oxidant during the wastewater treatment. The reducing agent in the wastewater mainly consists of organic matter, and thus, the COD removal of AR 73 solution by the three different electrodes was applied to further evaluate the effect of the MWCNT modification of the electro-catalytic oxidation. Similarly, after 3 h of electrolysis, COD was decreased gradually to 45% by the Ti/ATONPs-MWCNTs electrodes, demonstrating the best performance for

COD removal. By contrast, the COD concentrations on Ti/ATONPs and Ti/SnO₂-Sb electrodes were decreased to 60% and 76%, respectively. Herein, the Ti/ATONPs-MWCNTs electrodes showed the best performance for the degradation of organic matter in the dye wastewater, according to the results for the degradation rate of AR 73 presented above.

In addition, the instantaneous current efficiency (ICE), representing the ratio of the current effectively employed at a given time to the applied current, was obtained according to [37]:

$$ICE = \frac{COD_t - COD_{t+\Delta t}}{8I\Delta t} FV \times 100\% \quad (3)$$

where COD_t is the experimental value at the given time t , $COD_{t+\Delta t}$ is the value after a certain interval of Δt , I is the current(A), F is the Faraday constant ($96485 \text{ C}\cdot\text{mol}^{-1}$), and V is the sample volume (L).

Based on the COD results, the ICE results (inset of Figure 7) indicated that during the degradation, the use ratio was shown to be highest in Ti/ATONPs-MWCNTs, while it was the lowest in Ti/SnO₂-Sb, corresponding to the energy consumption results presented in the subsequent section. It can be concluded that Ti/ATONPs-MWCNTs electrodes show a steady efficiency of greater than 80% during the degradation process. The Ti/ATONPs-MWCNTs electrodes exhibit an outstanding current efficiency compared to the Ti/SnO₂-Sb/SnO₂-Sb-CNT electrodes fabricated by the pulse electrodeposition technique [38]. However, we can conclude that the removal of COD was less than the removal of concentration of AR 73 at the same interval through the results above, stating that other reducing agents were produced during the degradation—a result that requires further study.

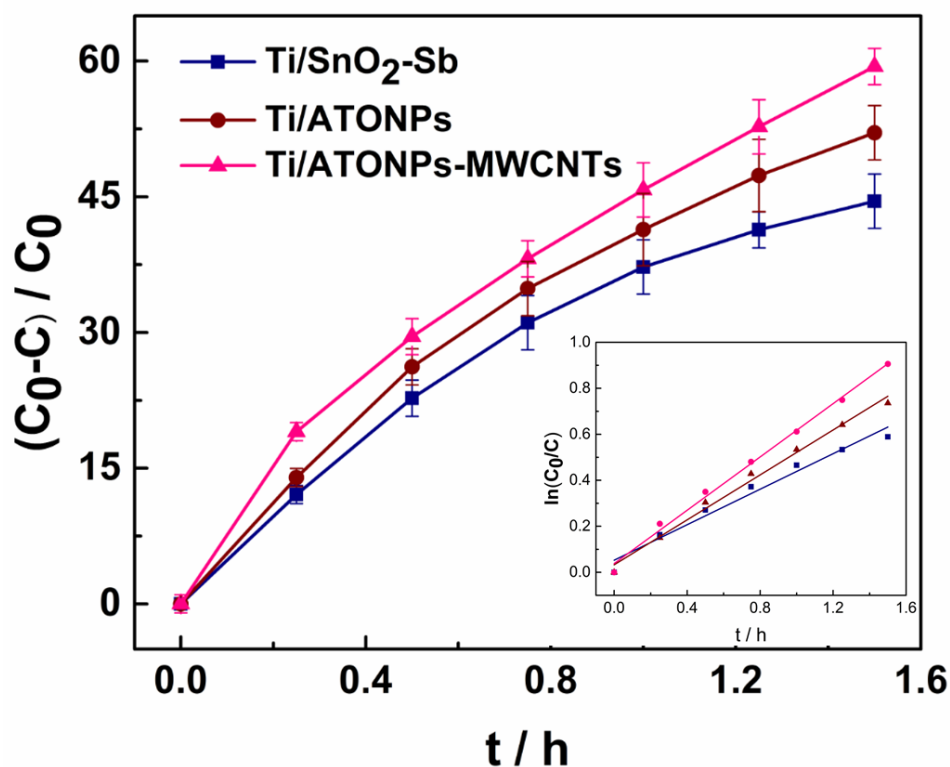


Figure 6. Chroma removal rate of AR 73 and semilog relationship of AR 73 chroma with the electrolysis time (inset). Conditions: $0.5 \text{ g}\cdot\text{L}^{-1}$ AR 73, 1.5 h at room temperature.

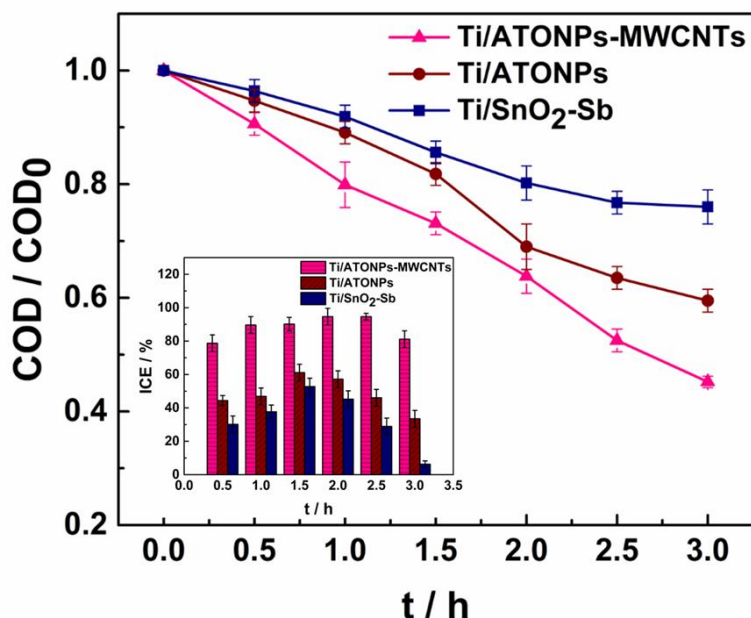


Figure 7. COD removal and Instantaneous current efficiency (ICE) on different electrodes. Conditions: $0.5 \text{ g}\cdot\text{L}^{-1}$ AR 73, 3 h at room temperature with current density of $20 \text{ mA}\cdot\text{cm}^{-2}$.

3.5. Energy consumption

The economic feasibility and applicability of AR 73 degradation by the Ti/ATONPs-MWCNTs, Ti/ATONPs and Ti/SnO₂-Sb electrodes were evaluated by determining the energy consumption. The performance of the electrodes could be compared by calculating the energy cost of the degradation to a given concentration. The energy consumption ($\text{Wh}\cdot\text{L}^{-1}$) can be determined as:

$$E = \frac{S \times i \times U}{V} t \quad (4)$$

where E is the specific energy consumption ($\text{Wh}\cdot\text{L}^{-1}$), S is the actual surface area of the anodes (cm^2), I is the applied current density ($\text{mA}\cdot\text{cm}^{-2}$), V is the volume of the solution in the reactor (L), and the average cell potential U was 4.9 V, 5.1 V and 5.3 V for Ti/ATONPs-MWCNTs, Ti/ATONPs and Ti/SnO₂-Sb electrodes, respectively, during the electrolysis process. The time (t) corresponding to the given concentration, was calculated by the k values determined from the data presented in the electrochemical oxidation section following the pseudo-first-order kinetics since this could simulate the treatment of wastewater in the real condition. The following equation was used to determine the time (t):

$$t = -\frac{1}{k} \ln \frac{C_t}{C_0} \quad (5)$$

where t (min) is the time needed to degrade AR 73 to a given concentration, k (min^{-1}) is the first-order rate constant, C_0 is the initial concentration of AR 73, and C_t is the concentration of AR 73 at a given time ($\text{mg}\cdot\text{L}^{-1}$).

To contrast the economic feasibility of AR 73 degradation by the three electrodes, data for energy consumption of degradation to a given concentration are presented in Figure 8. The electrodes fabricated by screen printing consumed less energy than the electrodes fabricated by electrochemical deposition. Moreover, compared to Ti/ATONPs, the energy consumption of the electrode modified

with MWCNTs (Ti/ATONPs-MWCNTs) showed a further decrease, corresponding to the results described above. When the removal of AR 73 reached 80%, the energy consumption of Ti/ATONPs-MWCNTs decreased by almost 19% and 40% relative to Ti/ATONPs and Ti/SnO₂-Sb electrodes, respectively. Due to the addition of MWCNTs and the use of screen printing, Ti/ATONPs-MWCNTs had both the porous structure of MWCNTs and the nano-sized grains of ATONPs, thus enabling the fabrication of a kind of electrode with the low energy consumption. Therefore, the Ti/ATONPs-MWCNTs electrode shows economic rationality and applicability to wastewater treatment by electrocatalytic oxidation.

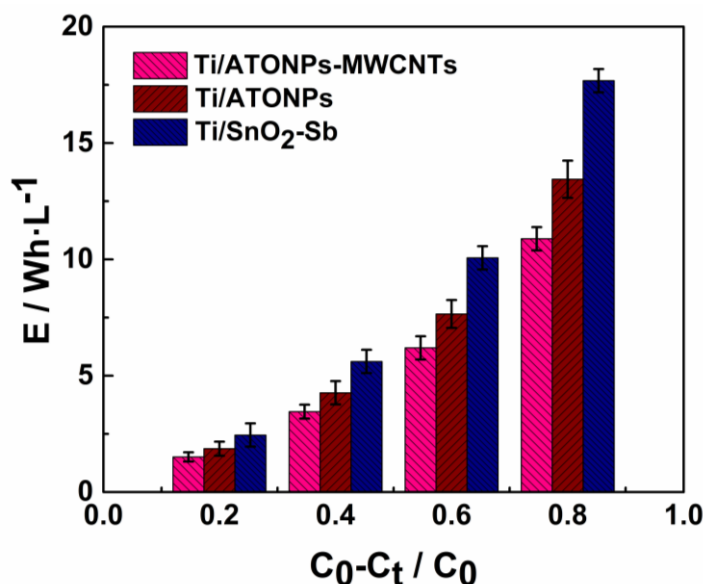


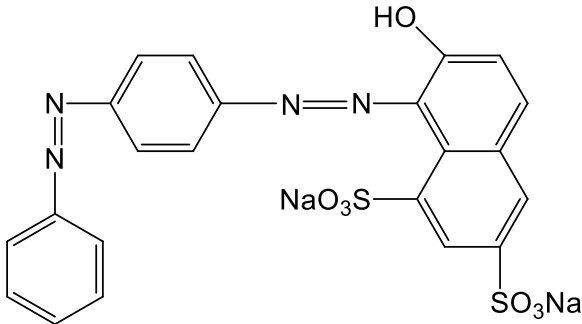
Figure 8. Evolution of energy consumption for degrading Acid Red 73 at a given concentration for different electrodes

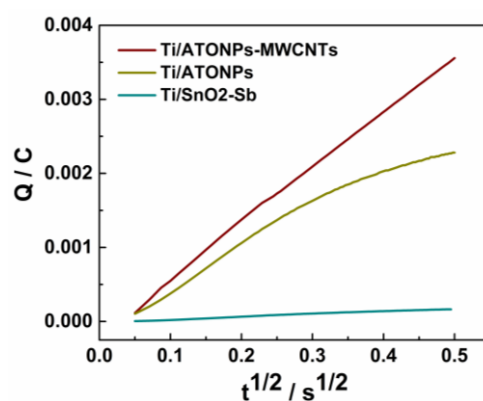
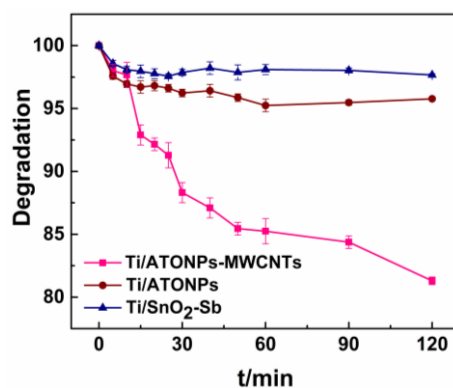
4. CONCLUSIONS

A novel Ti/ATONPs-MWCNTs electrode has been successfully fabricated by the screen-printing technique. Unlike the traditional Ti/SnO₂-Sb electrode prepared by electrochemical deposition and original Ti/ATONPs electrode prepared by screen printing, Ti/ATONPs-MWCNTs electrode has the combination of nano-sized grains and tubular porous structure enabling the formation of a comparatively larger electrochemically effective surface area. Addition of MWCNTs enhanced the electrical conductivity, resulting in the decreased electrochemical impedance and increased specific capacitance. Moreover, the electrode modified with MWCNTs shows better physical adsorption without the electric current. This advantage enables its better energy conservation performance. After 90 min of electrolysis, the removal efficiency of AR 73 reached 59.4% with the energy consumption of nearly 6.2 Wh·L⁻¹. Additionally, the remnant chemical oxygen demand (COD) was only 45% after 3 h degradation with the instantaneous current efficiency (ICE) greater than 80%. In summary, the novel Ti/ATONPs-MWCNTs electrode shows an excellent performance in wastewater treatment on the basis of all the results discussed above, providing some new insight into the industrial applications of electrochemical technology.

SUPPORTING INFORMATION:

Table S1. Characteristics of C.I. Acid Red 73.

Characteristics	C.I. Acid Red 73
Molecular formula	$C_{22}H_{14}N_4Na_2O_7S_2$
Molecular weight	556.490
λ_{\max} (nm)	518
CAS Number	5413 - 75 - 2
Corlor Index Number	27290
Molar volumes (mM^{-1})	323.5
Molecular structure	

**Figure S1.** The plot of $Q-t^{1/2}$ curve in chronocoulometry measurement by 0.1 mM $K_3[Fe(CN)_6]$ containing 1 M KCl.**Figure S2.** Degradation of AR 73 during the physical adsorption processes of different electrodes. Condition: 0.1 g·L⁻¹ AR 73, 2 h at room temperature.

NOTES

The authors declare no competing financial interest.

ACKNOWLEDGEMENTS

Our research was supported by the Nation Natural Science Foundation of China (Grand No.21276177)

References

1. G. Mezohegyi, F. Gonçalves, J.J.M. Órfão, A. Fabregat, A. Fortuny, J. Font, C. Bengoa, F. Stuber, *Appl. Catal. B-Environ.* 94 (2010) 179-185.
2. K.P. Sharma, S. Sharma, S. Sharma, P.K. Singh, S. Kumar, R. Grover, P.K. Sharma, *Chemosphere* 69 (2007) 48-54.
3. C.A. Martínez-Huitle, E. Brillas, *Appl. Catal. B-Environ.* 87 (2009) 105-145.
4. A. Sahoo, S.K. Tripathy, N. Dehury, S. Patra, *J. Mater. Chem. A* 3 (2015) 19376-19383.
5. W. Wu, Z.-H. Huang, T.-T. Lim, *Appl. Catal. A-Gen.* 480 (2014) 58-78.
6. A.N.S. Rao, V.T. *Environ. Sci. Pollut. Res.* 21 (2014) 3197-3217.
7. E. Chatzisyneon, S. Fierro, I. Karafyllis, D. Mantzavinos, N. Kalogerakis, A. Katsaounis, *Catal. Today* 151 (2010) 185-189.
8. M. Govindaraj, M. Muthukumar, G.B. Raju, *Environ. Technol.* 31 (2010) 1613-1622.
9. S. Ai, M. Gao, W. Zhang, Q. Wang, Y. Xie, L. Jin, *Talanta* 62 (2004) 445-450.
10. X. Duan, Y. Zhao, W. Liu, L. Chang, X. Li, *J. Taiwan Inst. Chem. E.* 45 (2014) 2975-2985.
11. F. Zaviska, P. Drogui, J.F. Blais, G. Mercier, P. Lafrance, *J. Hazard. Mater.* 185 (2011) 1499-1507.
12. B.N. Bhadra, P.W. Seo, S.H. *Chem. Eng. J.* 301 (2016) 27-34.
13. S. Sun, Y. Wang, G. Ding, H. Wang, *Environ. Sci. Technol.* 34 (2011) 159-162.
14. L. Zuo, Y. Guo, X. Li, X. Qu, S. Zheng, C. Gu, D. Zhu, P.J.J. Alvarez, *Environ. Sci. Technol.* 50 (2016) 899-905.
15. J.-W. Yoon, S. H. Choi, J.-S. Kim, H. W. Jang, Y. Kang, J.-H. Lee, *NPG Asia Mater.* 8 (2016) e244-e252.
16. T. Duan, Q. Wen, Y. Chen, Y. Zhou, Y. Duan, *J. Hazard. Mater.* 280 (2014) 304-314.
17. P. Duverneuil, F. Maury, N. Pebere, F. Senocq, H. Vergnes, *Surf. Coat. Technol.* 151 (2002) 9-13.
18. Y. Lu, Z. Tu, L. A. Archer, *Nat. Mater.* 13 (2014) 961-969.
19. J. Fang, L. Schlag, S. C. Park, T. Stauden, J. Pezoldt, P. Schaaf, H.O. Jacobs, *Adv. Mater.* 28 (2016) 1770-1779.
20. S. C. Warren, M. R. Perkins, A. M. Adams, M. Kamperman, A. A. Burns, H. Arora, E. Herz, T. Suteewong, H. Sai, Z. Li, J. Werner, J. Song, U. W. Zwanziger, J. W. Zwanziger, M. Grätzel, F. J. DiSalvo, U. Wiesner, *Nat. Mater.* 11 (2012) 460-467.
21. L. Zhang, L. Xu, J. He, J. Zhang, *Electrochim. Acta* 117 (2014) 192-201.
22. L. Xu, X. Song, *Electrochim. Acta* 185 (2015) 6-16.
23. P.L. Taberna, S. Mitra, P. Poizot, P. Simon, J.M. Tarascon, *Nat. Mater.* 5 (2006) 567-573.
24. H. Yin, Q. Ma, Y. Zhou, S. Ai, L. Zhu, *Electrochim. Acta* 55 (2010) 7102-7108.
25. R. Verdejo, C. Saiz-Arroyo, J. Carretero-Gonzalez, F. Barroso-Bujans, M.A. Rodriguez-Perez, M.A. Lopez-Manchado, *Eur. Polym. J.* 44 (2008) 2790-2797.
26. W. Wu, Z.-H. Huang, T.-T. Lim, *RSC Advances* 5 (2015) 32245-32255.
27. F. Wang, S. Li, M. Xu, Y. Wang, W. Fang, X. Yan, *J. Electrochem. Soc.* 160 (2013) D53-D59.
28. J. Bisquert, G. Garcia-Belmonte, F. Fabregat-Santiago, N. S. Ferriols, P. Bogdanoff, E. C. Pereira, *J. Phys. Chem. B* 104 (2000) 2287-2298.
29. J. Ma, B. Li, H. Du, C. Xu, F. Kang, *J. Solid State Electr.* 16 (2012) 1353-1362.

30. Y. Duan, Y. Chen, Q. Wen, T. Duan, *J. Electroanal. Chem.* 768 (2016). 81-88.
31. O. Simond, V. Schaller, C. Comninellis, *Electrochim. Acta* 42 (1997) 2009-2012.
32. H. Huang, S. Yang, V. Robert, X. Wang, P.M. Ajayan, *Adv. Mater.* 26 (2014) 5160-5165.
33. L. Bao, J. Zang, X. Li, *Nano Lett.* 11 (2011) 1215-1220.
34. F. Anson, *Anal. Chem.* 36 (1964) 932-934.
35. P. Deng, Z. Xu, R. Zeng, C. Ding, *Food Chem.* 180 (2015) 156-163.
36. K. Yang, B. Xing, *Environ. Pollut.* 145 (2007) 529-537.
37. L. Xu, Z. Guo, L. Du, J. He, *Electrochim. Acta* 97 (2013) 150-159.
38. W. Wu, Z. Huang, Z. Hu, C. He, T. Lim, *Sep. Purif. Technol.* 179 (2017) 25-3

© 2018 The Authors. Published by ESG (www.electrochemsci.org). This article is an open access article distributed under the terms and conditions of the Creative Commons Attribution license (<http://creativecommons.org/licenses/by/4.0/>).